Feasibility Study for an Airborne N_2O Lidar

Christoph Kiemle, Andreas Fix, Christian Fruck, Martin Wirth
Institut für Physik der Atmosphäre, Deutsches Zentrum für Luft- und Raumfahrt (DLR)
D-82234 Oberpfaffenhofen, Germany
Lead Author e-mail address: Christoph.Kiemle@dlr.de

Abstract: Nitrous oxide, N_2O is the third most important anthropogenic greenhouse gas after carbon dioxide and methane. The major source is nitrogen fertilization in croplands. Differential absorption lidar is very demanding since suitable absorption lines exist only in the infrared, which challenges lidar transmitter and detector options. Spectroscopic investigations and lidar instrumental noise simulations show that in the 4.5 µm band a trough position between two strong N_2O lines is likely the best option for an airborne lidar. A second option exists in the 3.9 µm band, at the cost of higher laser frequency stability constraints. Independently on the 3.9 versus 4.5 µm question an airborne lidar is expected to fulfill the N_2O measurement requirements for regional gradient or hot spot detection with technically realizable and affordable transmitter (100 mW average laser power) and receiver (20 cm telescope) characteristics. However, such a system would benefit from progress in infrared transmitter and detector technology.

1. Introduction

Nitrous oxide, N_2O is the third most important greenhouse gas contributing to human-induced global warming after carbon dioxide and methane. Albeit its atmospheric concentration amounts to only 0.336 ppm its global warming potential is 270 times that of CO_2 on a 100-year span [1]. The major anthropogenic source is nitrogen fertilization in croplands. Soil N_2O emissions are increasing due to interactions between nitrogen inputs and global warming, constituting an emerging positive N_2O-climate feedback. The recent increase in global N_2O emissions exceeds even the most pessimistic emission trend scenarios developed by the IPCC, underscoring the urgency to mitigate N_2O emissions.

Estimating N_2O emissions from agriculture is inherently complex and comes with a high degree of uncertainty, due to variability in weather and soil characteristics, in agricultural management options and in the interaction of field management with environmental variables. Further sources of N_2O are processes in the chemical industry and combustion processes. The sink of N_2O in the stratosphere increases the NO_x concentration which catalytically depletes ozone. Better N_2O measurements are urgently needed, particularly by means of remote sensing.

Airborne (or future satellite) based N_2O lidar remote sensing combines the advantages of high measurement accuracy, large-area coverage and nighttime measurement capability. Past feasibility studies revealed that Integrated-Path Differential-Absorption (IPDA) lidar providing vertical column concentrations of N_2O would be the method of choice [2,3]. In the meantime, airborne IPDA lidar systems successfully measure CO_2 and CH_4 [4,5].

The infrared spectral region where suitable N_2O absorption lines exist, particularly challenges passive remote sensing by means of spectroscopy, but also lidar transmitter and detector technology options. On the transmitter side, the use of optical parametric conversion schemes looks promising, while HgCdTe avalanche photodiode (MCT APD) [6], superconducting nanowire single-photon (SNSPD) [7] or up-conversion detectors (UCD) [8,9] could offer high-efficiency, low-noise signal detection. These options are implemented into a lidar simulation model in order to identify the optimal system configuration for measuring N_2O from aircraft with the IPDA method.

The objective is to observe regional-scale N_2O gradients along the flight track attributable to different soil emission fluxes, as well as hot spot emission plumes from, e.g., fertilizer production sites. The lidar platform is assumed

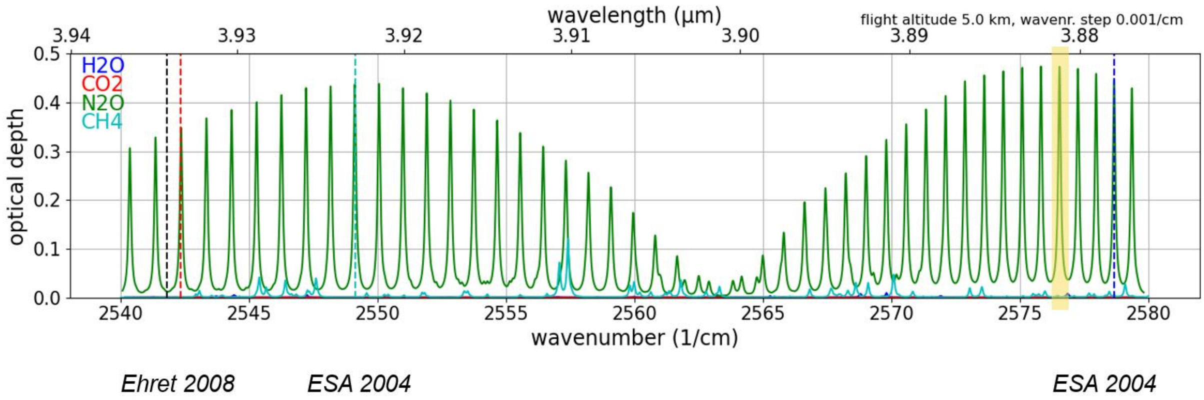

Figure 1. N_2O opt. depth in the 3.9 µm band.

to fly above the boundary layer in which N_2O surface emissions disperse vertically, and should measure with a precision of 0.5 %. This requirement is obtained from analyzing the magnitude of typical N_2O gradients measured by airborne in-situ instruments over various agricultural landscapes [10,11].

2. Spectroscopy

We use recent HITRAN spectroscopic data [12] to identify absorption lines of appropriate line strength in the rotational-vibrational N_2O bands centered at around 2.9, 3.9, 4.5 and 7.8 µm. The absorption cross sections are calculated with the Hartmann-Tran scheme [13] using standard atmosphere profiles of pressure, temperature and trace gas concentrations. Besides the line strength, additional line selection criteria are (a) low temperature sensitivity and (b) minimal interference with other gases. In this respect the entire 2.9 and 7.8 µm bands had to be excluded due to a ubiquitous presence of water lines, and also of methane lines at 7.8 µm. Therefore, we restricted ourselves to the 3.9 and 4.5 µm N_2O bands.

We assume an airborne lidar pointing vertically downward from a flight altitude of 5 km, well above the boundary layer. Figure 1 illustrates the one-way vertical column optical depth of the lowermost 5 km as function of wavenumber and wavelength, respectively. The optical depth is the vertically integrated product of the absorption cross section and the trace gas molecule number density. Both terms vary with height. Besides N_2O (green), water (blue), CO_2 (red) and CH_4 (cyan) need to be considered in this spectral region. Line selections from former satellite lidar studies [2,3] are indicated as vertical dotted lines with the references in the bottom.

Those selections are still valid for future spaceborne lidars, yet for airborne measurements at 5 km altitude all line strengths in this 3.9 µm band are suboptimal. One of the strongest lines, situated at 2576.5 cm^{-1}, is selected here (highlighted yellow in Figure 1). It is characterized by the absence of other absorbing gases and by low temperature sensitivity. The latter is determined by re-computing the spectra of optical depth for an atmosphere that is warmer by 1 K. The resulting difference in optical depth is directly proportional to the temperature sensitivity.

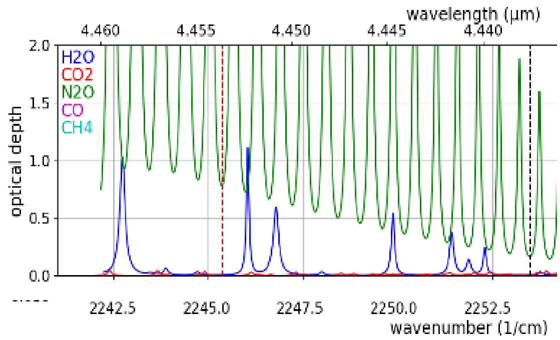

Figure 2. N_2O opt. depth in the 4.5 µm band.

The 4.5 µm band has much stronger N_2O lines. Here, a weaker line at the edge of the band may be selected, or a trough position in between two strong lines as utilized for CH_4 IPDA lidar [4]. In this study we select a trough position at the high-wavenumber side of the band, at 2245.4 cm^{-1} (Figure 2, red) because it is less influenced by other gases than the opposite side. The center of the band with weaker N_2O lines must be avoided due to water lines and due to elevated temperature sensitivity of the N_2O lines.

The trough position brings higher measurement sensitivity at low altitudes, i.e. near the surface where the N_2O sources are located, thanks to stronger pressure broadening. It also considerably relaxes the laser frequency stability requirement due to a relatively flat optical depth. Issues arise due to many strong neighboring lines whose wings influence the trough by superposition, and due to an offline wavelength required to be placed outside the band, at least 16 nm apart from the online position, marked as black dotted line at 2253 cm^{-1} in Figure 2. A large separation between on- and offline introduces biases if surface albedo or aerosol extinction are wavelength dependent. Since the albedo at these wavelengths is very low [15] the effect is possibly negligible. Table 1 summarizes the key advantages and disadvantages of both N_2O band alternatives.

Table 1. Tradeoff 3.9 versus 4.5 µm

N_2O Band	**3.9 µm**	**4.5 µm**
Online position	line center	wing / trough
Laser frequency stability	severe	relaxed
Measurement sensitivity	vertically neutral	peaks at surface
Offline position	0.5 nm apart	16 nm apart
Influence by close N_2O lines	weak	strong

3. N_2O Lidar Simulation

The optimal online optical depth depends, among other factors like flight altitude, on the level of instrumental noise [2,3], which was determined using a simple IPDA lidar simulation based on an atmospheric transmission and a detector model. The simulation serves to scale laser power and telescope size such as to fit the N_2O measurement precision requirement of 0.5 % for a flight altitude of 5 km and an along-track horizontal resolution of 500 m. In-situ airborne measurements [10,11] show that this resolution is sufficient to detect typical regional N_2O gradients. In order to detect smaller but denser N_2O hot spot plumes the horizontal resolution can be improved at the cost of precision.

Figure 3 shows the main simulation parameters and the resulting 1-sigma measurement noise (precision) as a function of (prescribed) online optical depth for the 3.9 (blue) and 4.5 µm (red) online spectral positions. The differential (online – offline) optical depth is 0.44 (0.63) at 3.9 (4.5) µm. For IPDA the surface albedo is the main environmental performance parameter. 0.02 can be considered a safe worst case [15]. The Planck equation yields an earth emission of 1.0 W/(m^2 sr µm) and a solar background radiation of 0.3 W/(m^2 sr µm), totaling 1.3 W/(m^2 sr µm). Extinction by rural aerosol is expected to add a one-way optical depth of 0.2. Using a mercury cadmium telluride (MCT) avalanche photodiode (APD) detector [14] with a noise equivalent power (NEP) of 0.1 pW/$Hz^{1/2}$ the optimum one-way optical depth for minimum noise is 1.0 (1.1) at 3.9 (4.5) µm.

Figure 1 shows that in the 3.9 µm band the optimum optical depth cannot be reached for a flight altitude of 5 km. On the other hand, the low offline optical depth leads to a satisfactory noise level. At 4.5 µm, a trough approaching the optimal optical depth could be found, as shown in Figure 2. With a resulting noise level of approximately 0.4 % at the 3.9 (4.5) µm optical depth selections the chosen configuration of Figure 3 fulfills all measurement requirements. The dashed lines show simulation results for an ideal noise-free detector where simply Poisson noise from laser and background photons is considered, for comparison. The gap to the APD detector may be reduced thanks to progress in detector development.

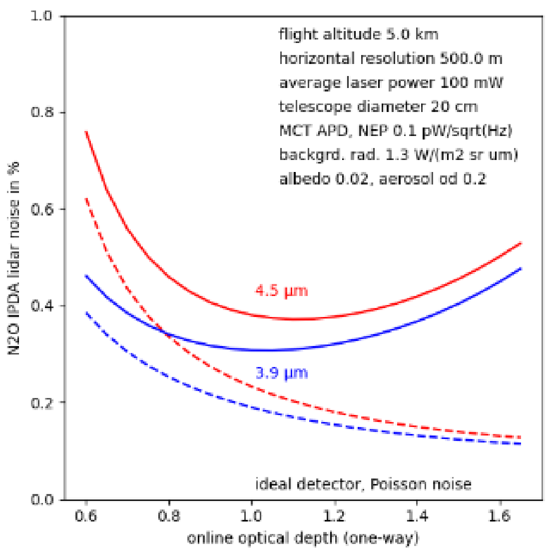

Figure 3. N_2O lidar noise simulation results.

4. Conclusions

Spectroscopic and instrument noise analyses show that a trough position in the 4.5 µm band is the best option for airborne N_2O IPDA lidar under the preconditions that the distant offline is uncritical and that the neighboring strong lines do not adversely influence wavelength positions in the trough other than line wing superposition already considered in the Hartmann-Tran calculations. The 3.9 µm alternative is the fallback option, coming at the cost of higher laser frequency stability constraints and less sensitivity to surface N_2O sources.

Independently on the 3.9 versus 4.5 µm question an airborne IPDA lidar is found to fulfill the N_2O measurement requirements for regional gradient or hot spot detection, with technically realizable and affordable transmitter (100 mW average laser power) and receiver (20 cm telescope) characteristics. Open questions concern various transmitter and detector options where technology is in progress.

5. References

[1] Arias, P.A. et al.: Technical Summary. In Climate Change 2021: The Physical Science Basis. Contribution of Working Group I to the Sixth Assessment Report of the Intergovernmental Panel on Climate Change. Cambridge University Press, Cambridge, United Kingdom and New York, USA, pp. 33−144. doi:10.1017/9781009157896.002.

[2] Ehret, G. and C. Kiemle: Requirements Definition for Future DIAL Instruments. ESA Study Final Report, ESA-CR(P)-4513 (2005).

[3] Ehret, G., C. Kiemle, M. Wirth, A. Amediek, A. Fix, and S. Houweling: Space-borne remote sensing of CO2, CH4, and N2O by integrated path differential absorption lidar: a sensitivity analysis. Appl. Phys. B **90**, 593-608 (2008).

[4] Amediek, A., Ehret, G., Fix, A., Wirth, M., Büdenbender, C., Quatrevalet, M., Kiemle, C., and Gerbig, C.: CHARM-F - a new airborne integrated-path differential-absorption lidar for carbon dioxide and methane observations: measurement performance and quantification of strong point source emissions. Applied Optics, **56** (18), 5182-5197. DOI: 10.1364/AO.56.005182 (2017)

[5] Mao, J., Abshire, J. B., Kawa, S. R., Sun, X., and Riris, H.: Airborne lidar measurements of atmospheric CO2 column concentrations to cloud tops made during the 2017 ASCENDS/ABoVE campaign, Atmos. Meas. Tech., 17, 1061–1074, https://doi.org/10.5194/amt-17-1061-2024, (2024).

[6] Nehrir, A., Kiemle, C., Lebsock, M. D. Kirchengast, G., Buehler, S. A., Löhnert, U., Liu, C-L., Hargrave, P. C., Barrera Verdejo, M., Winker, D. M.: Emerging Technologies and Synergies for Airborne and Space-Based Measurements of Water Vapor Profiles. Surveys in Geophysics, **38**, 1445-1482 DOI: 10.1007/s10712-017-9448-9. (2017)

[7] Charaev, I., et al.: Single-photon detection using high-temperature superconductors. Nature Nanotechnol. **18**, 343-349 (2023).

[8] Hoegstedt, L., Fix, A., Wirth, M., Pedersen, C., Tidemand-Lichtenberg, P.: Upconverion-based lidar measurements of atmospheric CO2. Optics Express **24**, 5 (2016). DOI:10.1364/OE.24.005152

[9] Meng, L., Fix, A., Wirth, M., et al.: Upconversion detector for range-resolved DIAL measurement of atmospheric CH4. Optics Express **26**, 4, (2018).

[10] Eckl, M., Roiger, A., Kostinek, J., Fiehn, A., Huntrieser, H., Knote, C., Barkley, Z. R., Ogle, S., Baier, B. C. Sweeney, C. and Davis, K. J.: Quantifying nitrous oxide emissions in the U.S. Midwest - A top-down study using high resolution airborne in situ observations. GRL, **48** (5), (2021), e2020GL091266. doi: 10.1029/2020GL091266

[11] Waldmann, P., et al.: Quantifying agricultural CH4 and N2O emissions of the Netherlands using a novel airborne eddy-covariance measurements system: First results of the GHGMon campaign in June 2023. EGU24-19467. General Assembly of the European Geosciences Union, Vienna, April 2024.

[12] Gordon, I. E., et al.: The HITRAN2020 molecular spectroscopic database. JQSRT **277** (2022).

[13] N.H. Ngo, D. Lisak, H. Tran, J.-M. Hartmann: An isolated line-shape model to go beyond the Voigt profile in spectroscopic databases and radiative transfer codes. JQSRT, **129**, 89–100. http://dx.doi.org/10.1016/j.jqsrt.2013.05.034 (2013)

[14] Beck, J., C. Wan, M. Kinch, J. Robinson, P. Mitra, R. Scritchfield, F. Ma, J. Campbell: The HgCdTe Electron Avalanche Photodiode. IEEE Lasers and Electro-Optics Society Newsletter p. 8-12, Oct. 2006.

[15] ECOSTRESS (Ecosystem Spaceborne Thermal Radiometer Experiment on Space Station; formerly ASTER) spectral library. https://speclib.jpl.nasa.gov/library